

Nanofibre-assisted alignment of carbon nanotubes in macroscopic polymer matrix via a scaffold-based method

Z. J. Chang¹, X. Zhao¹, Q. H. Zhang¹, D. J. Chen^{1,2*}

¹State Key Laboratory for Modification of Chemical Fibers and Polymer Materials Shanghai 201620, People's Republic of China

²College of Materials Science and Engineering, Donghua University Shanghai 201620, People's Republic of China

Received 19 September 2009; accepted in revised form 28 October 2009

Abstract. A facile way for alignment of carbon nanotubes in macroscopic polymer matrix was developed by combining electrospinning and *in-situ* polymerization. The approach is based on the formation of nanofibre scaffolds with well-aligned arrays, which is filled with carbon nanotubes (CNTs). CNTs will be well aligned in macroscopic polymer matrix when the aligned nanofibre scaffold containing CNTs has been incorporated into the poly(methyl methacrylate) (PMMA) matrix by *in-situ* polymerization. We demonstrate that this scaffold approach is broadly applicable and allows for the fabrication of nanocomposites with accurately aligned nanofillers. The results presented in this report show that the approach is ideal by using polyacrylonitrile (PAN) nanofibres as a scaffold of multiwalled carbon nanotubes (MWNTs), and PMMA as the macroscopic polymer matrix. The tensile strength (7.2 wt% MWNTs/PAN nanofibres loadings) reaches 48.61 MPa, 87% higher than that pure PMMA, and the tensile modulus is increased by 175%.

Keywords: nanocomposites, electrospinning, nanofibres, carbon nanotubes, alignment

1. Introduction

Carbon nanotubes (CNTs) possess high intrinsic strength, stiffness, flexibility, high thermal and electrical conductivity, and are being incorporated in polymers to obtain composites with unique properties. Since the discovery of CNTs by Iijima [1], carbon nanotube-based polymer composites have become a focal point of nanocomposite research [2–4].

The state of dispersion, alignment, assembly and load stress transfer of CNTs is crucially important to the performance of nanocomposites [5]. Because of their small size, CNTs usually have high specific surface areas, resulting in a strong tendency for aggregation, so it is difficult to assemble them in polymer matrix. The dispersion and alignment of CNTs in macroscopic polymer matrix are the bigger challenges for the development of polymer

nanocomposites. Over the past years, many groups have studied the dispersion of CNTs in various polymer matrices. Several processing methods are available for producing nanotube/polymer composites include: melt-mixing, solution processing, *in-situ* polymerization, gelation/crystallization method. Although these methods are different, all of them try to disperse CNTs in polymer matrix.

Electrospinning is a highly versatile method for processing solutions or melts, mainly of polymers, into continuous fibres with diameters ranging from nano- to microscale. Like nanofillers mentioned above, nanofibres also show several amazing several characteristics such as surface area to volume ratio, flexibility in surface functionalities, and superior mechanical performance compared with conventional fibres. However, the aspect ratio of nanofibres is much larger than that of general

*Corresponding author, e-mail: cdj@dhu.edu.cn
© BME-PT

nanofillers which makes its assembling much easier. This outstanding property makes nanofibres to be optimal candidates for many important applications, including reinforcement, tissue engineering, energy and environment. In the previous research, pure random electrospun nanofibres tended to display enhanced mechanical properties in polymer matrix [6, 7]. Recently, polymer nanofibres containing carbon nanotubes [8–11], clay [12, 13], ceramics [14] and metals [15, 16] have been fabricated by several research groups. At the same time, research on nanofibre assemblies explored various structures and methods, including aligned fibres [17–20], patterned fibres [21, 22], and helical fibres [23].

In this report, we developed a general approach for the creation of polymer nanocomposites with alignment of CNTs. The processing scheme showed the initial fabrication process of the aligned polymer nanofibres with CNTs via controlled deposition of electrospun nanofibres. The polymer nanofibres become a scaffold of CNTs. CNTs will be confined in nanofibre environments, and can be aligned in nanofibre axial direction. This scaffold containing well aligned CNTs was immersed in the monomer solution. Then, the intended nanocomposite was obtained by *in-situ* polymerization. After polymerization, CNTs can be aligned within macroscopic polymer matrix. The approach, which is much easier than that in the previous methods, has a broad application and allows for the fabrication of materials with good thermal and mechanical properties. To examine the approach being facile, we used aligned polyacrylonitrile (PAN) nanofibres as a scaffold of multiwalled carbon nanotubes (MWNTs)

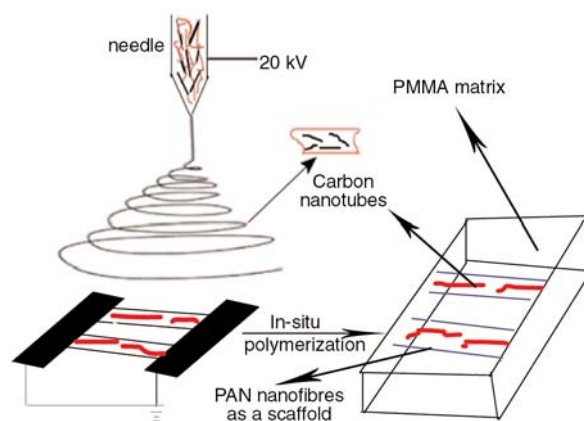


Figure 1. Alignment of MWNTs in PMMA matrix by a nanofibre scaffold

to fabricate aligned MWNTs/PAN composite nanofibres (ACNs) firstly, and then used poly(methyl methacrylate) (PMMA) as the macroscopic polymer matrix of ACNs. Schematics of the process are shown in Figure 1.

2. Experimental section

2.1. Materials

MWNTs with a purity of >95% were supplied from Shenzhen Nanotech Port Co. Ltd, China. Triton X-100, t -Oct- $C_6H_4-(OCH_2CH_2)_nOH$ ($n = 9-10$), was purchased from Aldrich. HNO_3 , $SOCl_2$ and dimethyl formamide (DMF) were purchased from Sinopharm Chemical Reagent Co. Ltd, China. The monomer, methyl methacrylate (MMA), 2,2'-azobisisobutyronitrile (AIBN) as the initiator and methanol were purchased from Sinopharm Chemical Reagent Co. Ltd, China. The AIBN was purified by re-crystallization from methanol before use. The other chemicals were used directly without further purification.

2.2. Electrospun MWNTs/PAN composite nanofibres

The MWNTs/PAN composites nanofibres were prepared according to the reported procedures [24]. The synthesis procedure can be briefly described as follows: MWNTs were functionalized by a mixture of concentrated sulfuric and nitric acids (3:1, by volume). As a result, many carboxylic acid groups ($-COOH$) were created in MWNTs. Then, the MWNT- $COOH$ mixture was suspended in $SOCl_2$ and stirred for 24 h at $65^\circ C$ to produce MWNT- $COCl$. The above MWNT- $COCl$ and Triton X-100 was stirred under N_2 atmosphere at $120^\circ C$ for 48 h. The MWNT-Triton (f-MWNTs) was thus obtained after washing and drying. For the fabrication of PAN/f-MWNT solution, 0.38 g of PAN (average molecular weight 70 000) and 0.02 g of MWNT-Triton were separately dissolved in 5 ml of DMF, and then the above solutions were mixed using an ultrasonicator. Well-aligned composite nanofibres containing PAN and f-MWNTs were prepared by electrospinning in dimethyl formamide solution, and a collector consisting of two parallel copper sheets was used to catch the nanofibres. The distance between parallel electrodes is 4 cm.

2.3. Preparation of polymer nanocomposites

MMA and purified AIBN were mixed together (20 ml of MMA:0.05 g of AIBN). A portion of the above solution was added to a glass mold. Then the nanofibre scaffold with the isolated MWNTs, which were well aligned along the nanofibre axes, was gently immersed in the solution. The mold was sealed with argon balloons after nitrogen was purged for 10 min. The polymerization was carried out in a water bath at 90°C for 15 min. Then it was polymerized at 55°C, for 16 h. After polymerization, the mold was broken. The PMMA/ACNs nanocomposites were taken out and cut some fringe sections, which did not contain ACNs.

2.4. Characterization

Thermogravimetric analysis (TGA) measurements were performed on Netzsch STA 490 under a nitrogen atmosphere from room temperature to 500°C. Wide angle X-ray diffraction (WAXD) intensity profiles of the sample were recorded with a diffractometer (D/Max-2550 PC, Rigaku, Japan). The molecular weight and molecular weight distributions of PMMA matrix from composite, using GPC (BI-MwA from Waters, LS). The solution was made by dissolving the samples in high-pressure liquid chromatography (HPLC)-grade tetrahydrofuran (THF) and filtered twice through 0.2 µm filters. The morphology and the alignment of the nanofibre scaffold in matrix were observed on a JSM-5600LV scanning electron microscope at an accelerating voltage of 10 kV, gold-sputtered prior to observation. The embedding and morphology of MWNTs within the nanofibres was measured on a Hitachi H-800 transmission electron microscope at 250 kV. Tensile tests were carried out on a Universal material testing machine (DXL-2000) at room temperature with a crosshead speed of 0.5 mm/min. The specimen gauge length was 4 cm and the width was 0.5 cm. In all cases, five samples were tested from which the standard deviations were calculated. The humidity of the laboratory was about 65%.

3. Results and discussion

MWNTs were functionalized by grafting Triton X-100 on their surface to improve their dispersion

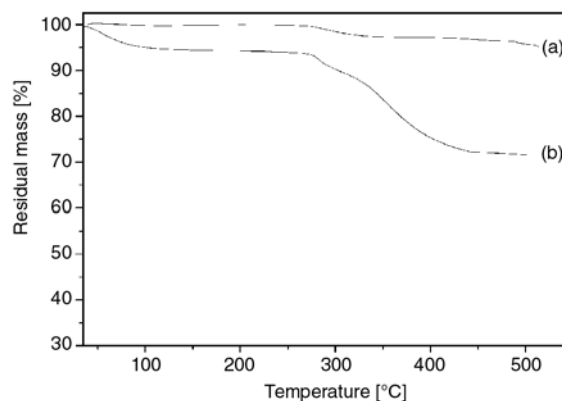


Figure 2. TGA of MWNTs (a) and MWNTs with grafted Triton X-100 (b)

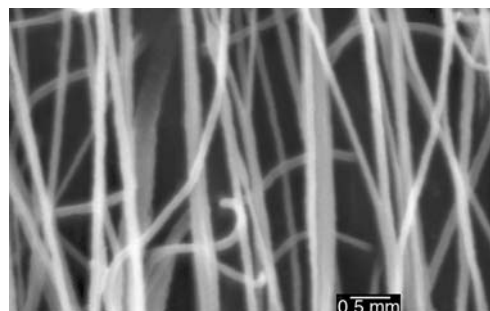


Figure 3. SEM images of the uniaxially aligned nanofibres with MWNTs

in the solution of PAN. The grafting yield is about 25 wt% by TGA data (Figure 2). Well-aligned composite nanofibres containing PAN with f-MWNTs were prepared by electrospinning in dimethyl formamide solution, and a collector consisting of two pieces of electrode was used to catch the nanofibres. SEM was used to observe the morphology of the nanofibres. Figure 3 shows the uniaxially aligned nanofibres. Figure 4 showed TEM images of the composite nanofibres in which the surface functionalized MWNTs grafted with Triton X-100 are embedded within the PAN nanofibre matrix. TEM observation showed a MWNT was parallel and oriented along the axes of the nanofibre. To determine whether the nanofibres influence the polymerization process, the GPC results indicate that average M_w is $5.6 \cdot 10^5$, the polydispersity of PMMA matrix (~ 2.18), as to pure PMMA with the average M_w ($6.7 \cdot 10^5$) and polydispersity ($=1.82$). The addition of ACNs shows a lower average molecular weight and a larger distribution of molecular weights. It can be concluded from these results that ACNs influence the *in-situ* polymerization of PMMA, by changing the polydispersity and molecular weight.

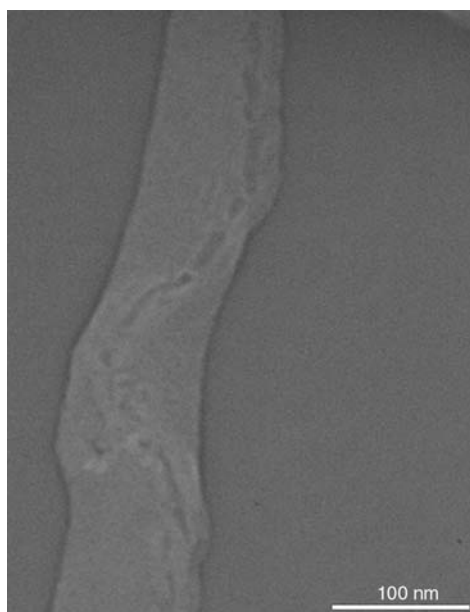


Figure 4. TEM image of nanofibre with well-oriented MWNT along the axis of nanofibre

The WAXD spectra obtained from electrospun pure aligned PAN nanofibre are presented in Figure 5a, where a characteristic diffraction peak at 16.8° and a weak peak at 28.7° were observed. These two peaks of diffraction can be assigned as (200) and (020) crystal planes of PAN. The composite sample (Figure 5b) showed a strong diffraction peak at 26.3° , was recognized as the diffraction of the (002) crystal planes of MWNTs. The weak peak is (101) at 44.3° . The result shows no significant difference from the diffraction pattern of composite nanofibres and pure PAN nanofibres, meaning that the 5 wt% f-MWNTs do not have much influence on the crystal morphology of PAN [9]. SEM was used to check the morphologies of ACNs in polymer matrix. In order to observe the morphology of ACNs in PMMA matrix, we stick them to

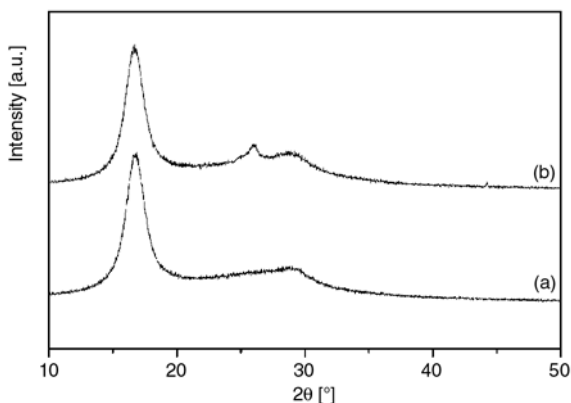


Figure 5. WAXD spectra of pure PAN nanofibres (a), and PAN-MWNTs composite nanofibres containing f-MWNTs of 5% by weight (b)

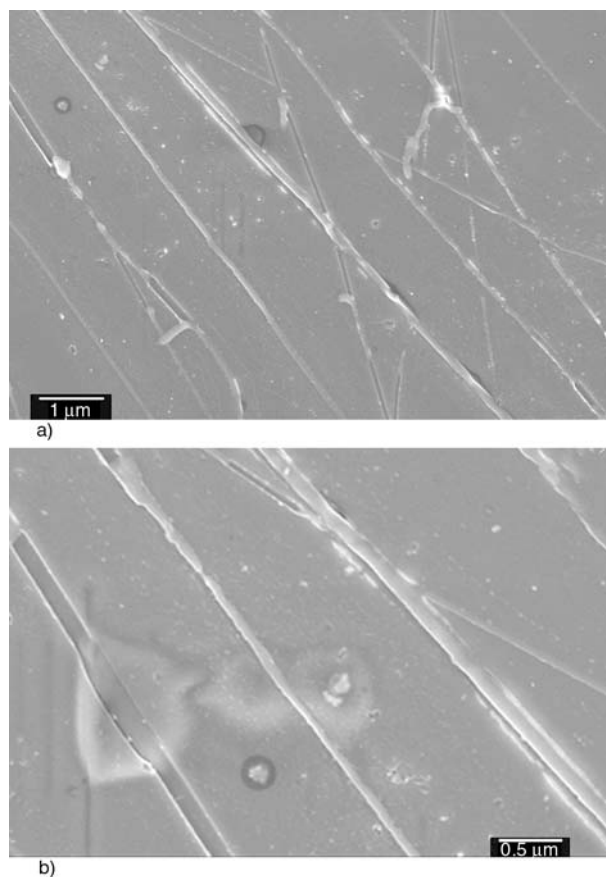


Figure 6. SEM images with different magnifications of the PMMA matrix with low-volume fraction of ACNs

bottom of the glass mold. Most of ACNs were embedded in matrix after *in-situ* polymerization. A part of ACNs embedded in polymer matrix from the bottom of the glass mold were exposed. Figure 6a gives an image with a low magnification of ACNs in PMMA matrix; a few of them are not parallel with the most of composite nanofibres but cross the ACNs. As shown in Figure 6b, the image with high magnification clearly shows that the ACNs are embedded in the PMMA matrix. Similar to existing macro-fibre composites, the ideal morphology nanocomposite has a high volume fraction of aligned, collinear nanotubes homogeneously dispersed in a surrounding matrix. By mechanically densifying ACNs, variable control of MWNTs volume fraction is easily obtained. Combined with polymer monomer into the nanofibre scaffold via simple capillarity-driven wetting along the axis of the MWNTs, nanocomposites are formed by *in-situ* polymerization. Figure 7a shows that the ultrahigh-volume-fraction ACNs were embedded in PMMA matrix. The clear morphology is shown by high magnification in Figure 7b.

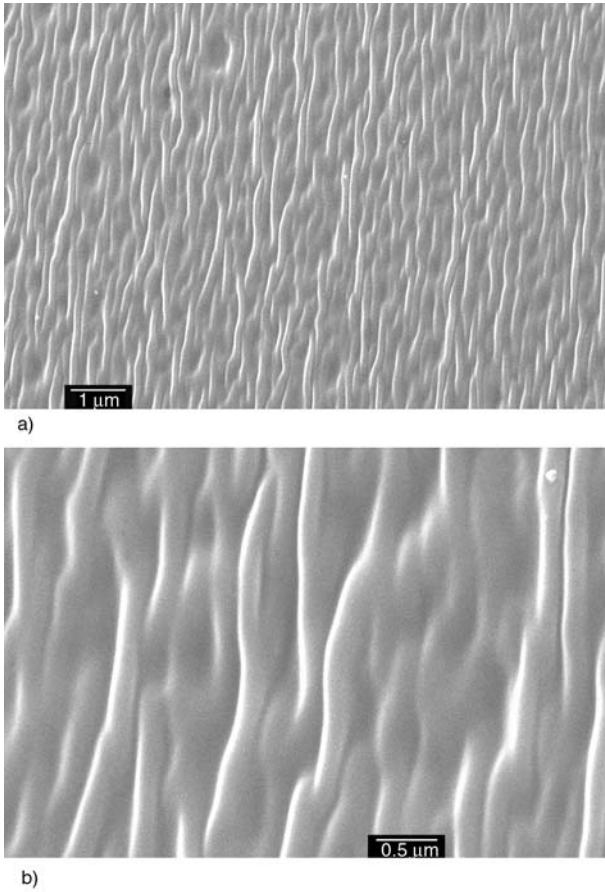


Figure 7. SEM images with different magnifications of the PMMA matrix with ultrahigh-volume fraction of ACNs

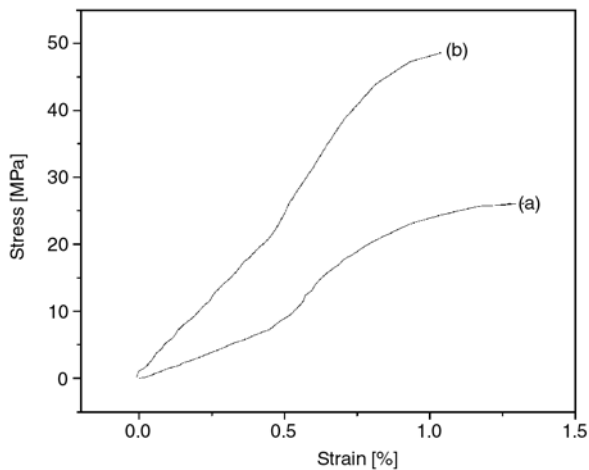


Figure 8. Stress–strain profiles of pure PMMA (a) and the composite with 7.2 wt% ACNs loadings (b)

Table 1. Tensile properties of PMMA and PMMA nanocomposites with ACNs

	Tensile strength [MPa]	Tensile modulus [GPa]	Strain at break [%]
Pure PMMA	26.04 ± 0.32	1.40 ± 0.21	1.29 ± 0.51
7.2 wt% ACNs	48.61 ± 0.75	3.86 ± 0.53	1.04 ± 0.37

Figure 8 shows the typical stress-strain curves of pure PMMA (a) and the PMMA/ACNs nanocomposites (b). The tensile strength, the tensile modulus and the strain at break values are summarized in Table 1. Pure PMMA shows a tensile strength of 26.04 MPa, and tensile modulus of 1.40 GPa, while the nanocomposite with the loading of ACNs (7.2 wt%) shows a strength of 48.61 MPa, and a tensile modulus of 3.86 GPa (axial direction of ACNs). This corresponds to an increase of about 87 and 175%, verifying the validity of introducing the aligned f-MWNTs as reinforcing fillers to PMMA matrix.

A wide variety of theoretical work has been carried out since the 1950s with the aim of modeling the mechanical properties of fibre-reinforced composites. There are the rule of mixtures and the Halpin-Tsai equations [25]. The Halpin-Tsai equation is used in the nanocomposites, which is known to fit some data very well at low volume fractions of fillers. In the equation, E_m is the tensile modulus of the matrix of ACNs, V_f is the MWNTs (in ACNs) volume fraction, l_f , d_f are length and diameter of MWNTs, respectively, l_f/d_f is the aspect ratio of MWNTs.

E_f of MWNT was taken as 450 GPa [26], whereas the volume fraction $V_f = 2.0\%$ was calculated from the measured weight fraction (5.0 wt%) of f-MWNTs, based on the MWNTs density (2.16 g/cm³), Triton X-100 density (1.07 g/cm³) and the PAN density (1.16 g/cm³). For the E_m , we use $E_m \approx 27$ GPa [27, 28]. The aspect ratio of MWNTs was 15, using measurements from transmission electron microscopy images. Since electrospun fibre formation imposes an axial orientation of the nanotubes, the composite modulus (E_{fibre}) can be calculated by Equation (1), resulting in a value of 38.8 GPa for ACNs containing 5 wt% f-MWNTs:

$$E_{fibre} = E_m \frac{1 + 2 \frac{l_f}{d_f} \eta V_f}{1 - \eta V_f} \quad (1)$$

where

$$\eta = \frac{\frac{E_f}{E_m} - 1}{\frac{E_f}{E_m} + 2 \frac{l_f}{d_f}} \quad (2)$$

The Halpin-Tsai equation is known to fit some data very well at low volume fractions but to underestimate stiffness at high volume fraction of nanofillers. The rule of mixtures can be used to model the ACNs/PMMA nanocomposites with high volume fraction of ACNs. In the simplest possible case a composite can be modeled as an isotropic, elastic matrix filled with aligned elastic fibres that span the full length of the specimen [29]. We use the rule of mixtures modeling properties of ACNs reinforced composites by Equation (3), where E_{fibre} is the ACNs modulus, E'_m is the matrix modulus, and V'_f is the ACNs volume fraction:

$$E_c = (E_{\text{fibre}} - E'_m)V'_f + E'_m \quad (3)$$

In Equation (3), E'_m of PMMA was taken as 1.40 GPa from experiment data, and the volume fraction $V'_f = 7.1\%$ was calculated from the measured weight fraction (7.2 wt%) of ACNs, based on ACNs weight put into the reacting solution and the PMMA density (1.17 g/cm³). The calculated modulus ($E_c = 4.05$ GPa) is close agreement with the experimental modulus (3.86 GPa), which indicates f-MWNTs are isolated and aligned in PMMA matrix.

4. Conclusions

In conclusion, the aligned PAN nanofibre scaffold containing MWNTs was introduced to PMMA matrix to control the alignment of MWNTs in PMMA matrix. MWNTs can be well aligned within macroscopic PMMA matrix via a scaffold of aligned PAN nanofibres. The reinforcement effect of ACNs has been clearly demonstrated. The approach can be broadly used for the fabrication of nanocomposites with better alignment and much higher volume fraction of nanofillers.

Acknowledgements

This work has been supported by the Fund of Innovation Project on Doctoral Dissertation of Donghua University and Supported by the Programme of Introducing Talents of Discipline to Universities (111-2-04).

References

- [1] Iijima S.: Helical microtubules of graphitic carbon. *Nature*, **354**, 56–58 (1991). DOI: [10.1038/354056a0](https://doi.org/10.1038/354056a0)
- [2] Moniruzzaman M., Winey K. I.: Polymer nanocomposites containing carbon nanotubes. *Macromolecules*, **39**, 5194–5205 (2006). DOI: [10.1021/ma060733p](https://doi.org/10.1021/ma060733p)
- [3] Zhang Q. H., Rastogi S., Chen D. J., Lippits D., Lemstra P. J.: Low percolation threshold in single-walled carbon nanotube/high density polyethylene composites prepared by melt processing technique. *Carbon*, **44**, 778–785 (2006). DOI: [10.1016/j.carbon.2005.09.039](https://doi.org/10.1016/j.carbon.2005.09.039)
- [4] Zhang Q. H., Lippits D. R., Rastogi S.: Dispersion and rheological aspects of SWNTs in ultrahigh molecular weight polyethylene. *Macromolecules*, **39**, 658–666 (2006). DOI: [10.1021/ma051031n](https://doi.org/10.1021/ma051031n)
- [5] Schaefer D. W., Justice R. S.: How nano are nanocomposites? *Macromolecules*, **40**, 8501–8517 (2007). DOI: [10.1021/ma070356w](https://doi.org/10.1021/ma070356w)
- [6] Bergshoef M. M., Vancso G. J.: Transparent nanocomposites with ultrathin, electrospun nylon-4,6 fiber reinforcement. *Advanced Materials*, **11**, 1362–1365 (1999). DOI: [10.1002/\(SICI\)1521-4095\(199911\)11:16<1362::AID-ADMA1362>3.0.CO;2-X](https://doi.org/10.1002/(SICI)1521-4095(199911)11:16<1362::AID-ADMA1362>3.0.CO;2-X)
- [7] Kim J-S., Reneker D. H.: Mechanical properties of composites using ultrafine electrospun fibers. *Polymer Composites*, **20**, 124–131 (1999). DOI: [10.1002/pc.10340](https://doi.org/10.1002/pc.10340)
- [8] Ayutsede J., Gandhi M., Sukigara S., Ye H. H., Hsu C. M., Gogotsi Y., Ko F.: Carbon nanotube reinforced *Bombyx mori* silk nanofibers by the electrospinning process. *Biomacromolecules*, **7**, 208–214 (2006). DOI: [10.1021/bm0505888](https://doi.org/10.1021/bm0505888)
- [9] Hou H. Q., Ge J. J., Zeng J., Li Q., Reneker D. H., Greiner A., Chen S. Z. D.: Electrospun polyacrylonitrile nanofibers containing a high concentration of well-aligned multiwall carbon nanotubes. *Chemistry of Materials*, **17**, 967–973 (2005). DOI: [10.1021/cm0484955](https://doi.org/10.1021/cm0484955)
- [10] McCullen S. D., Stevens D. R., Roberts W. A., Ojha S. S., Clarke L. I., Gorga R. E.: Morphological, electrical, and mechanical characterization of electrospun nanofiber mats containing multiwalled carbon nanotubes. *Macromolecules*, **40**, 997–1003 (2007). DOI: [10.1021/ma061735c](https://doi.org/10.1021/ma061735c)
- [11] Heikkilä P., Harlin A.: Electrospinning of polyacrylonitrile (PAN) solution: Effect of conductive additive and filler on the process. *Express Polymer Letters*, **3**, 437–445 (2009). DOI: [10.3144/expresspolymlett.2009.53](https://doi.org/10.3144/expresspolymlett.2009.53)

- [12] Ji Y., Li B. Q., Ge S. R., Sokolov J. C., Rafailovich M. H.: Structure and nanomechanical characterization of electrospun PS/clay nanocomposite fibers. *Langmuir*, **22**, 1321–1328 (2006).
DOI: [10.1021/la0525022](https://doi.org/10.1021/la0525022)
- [13] Kim G-M., Michler G. H., Ania F., Calleja F. J. B.: Temperature dependence of polymorphism in electrospun nanofibres of PA6 and PA6/clay nanocomposite. *Polymer*, **48**, 4814–4823 (2007).
DOI: [10.1016/j.polymer.2007.05.082](https://doi.org/10.1016/j.polymer.2007.05.082)
- [14] Shao C., Kim H-Y., Gong J., Ding B., Lee D-R., Park S-J.: Fiber mats of poly(vinyl alcohol)/silica composite via electrospinning. *Materials Letters*, **57**, 1579–1584 (2003).
DOI: [10.1016/S0167-577X\(02\)01036-4](https://doi.org/10.1016/S0167-577X(02)01036-4)
- [15] Lee H. K., Jeong E. H., Baek C. K., Youk J. H.: One-step preparation of ultrafine poly(acrylonitrile) fibers containing silver nanoparticles. *Materials Letters*, **59**, 2977–2980 (2005).
DOI: [10.1016/j.matlet.2005.05.005](https://doi.org/10.1016/j.matlet.2005.05.005)
- [16] Wang Y. Z., Li Y. X., Sun G., Zhang G. L., Liu H., Du J. S., Yang S. A., Bai J., Yang Q. B.: Fabrication of Au/PVP by electrospinning nanofiber composites by electrospinning. *Journal of Applied Polymer Science*, **105**, 3618–3622 (2007).
DOI: [10.1002/app.25003](https://doi.org/10.1002/app.25003)
- [17] Li D., Wang Y. L., Xia Y. N.: Electrospinning of polymeric and ceramic nanofibers as uniaxially aligned arrays. *Nano Letters*, **3**, 1167–1171 (2003).
DOI: [10.1021/nl0344256](https://doi.org/10.1021/nl0344256)
- [18] Matthews J. A., Wnek G. E., Simpson D. G., Bowlin G. L.: Electrospinning of collagen nanofibers. *Biomacromolecules*, **3**, 232–238 (2002).
DOI: [10.1021/bm015533u](https://doi.org/10.1021/bm015533u)
- [19] Teo W. E., Ramakrishna S.: Electrospun fibre bundle made of aligned nanofibres over two fixed points. *Nanotechnology*, **16**, 1878–1884 (2005).
DOI: [10.1088/0957-4484/16/9/077](https://doi.org/10.1088/0957-4484/16/9/077)
- [20] Theron A., Zussman E., Yarin A. L.: Electrostatic field-assisted alignment of electrospun nanofibres. *Nanotechnology*, **12**, 384–390 (2001).
DOI: [10.1088/0957-4484/12/3/329](https://doi.org/10.1088/0957-4484/12/3/329)
- [21] Li D., Ouyang G., McCann J. T., Xia Y. N.: Collecting electrospun nanofibers with patterned electrodes. *Nano Letters*, **5**, 913–916 (2005).
DOI: [10.1021/nl0504235](https://doi.org/10.1021/nl0504235)
- [22] Zhang D. M., Chang J.: Patterning of electrospun fibers using electroconductive templates. *Advanced Materials*, **19**, 3664–3667 (2007).
DOI: [10.1002/adma.200700896](https://doi.org/10.1002/adma.200700896)
- [23] Yu J., Qiu Y. J., Zha X. X., Yu M., Yu J. L., Rafique J., Yin J.: Production of aligned helical polymer nanofibers by electrospinning. *European Polymer Journal*, **44**, 2838–2844 (2008).
DOI: [10.1016/j.eurpolymj.2008.05.020](https://doi.org/10.1016/j.eurpolymj.2008.05.020)
- [24] Zhang Q. H., Chang Z. J., Zhu M. F., Mo X. M., Chen D. J.: Electrospun carbon nanotube composite nanofibres with uniaxially aligned arrays. *Nanotechnology*, **18**, 115611/1–115611/6 (2007).
DOI: [10.1088/0957-4484/18/11/115611](https://doi.org/10.1088/0957-4484/18/11/115611)
- [25] Mallick P. K.: *Fiber-reinforced composites: Materials, manufacturing, and design*. Marcell Dekker, New York (1993).
- [26] Liu L-Q., Tasis D., Prato M., Wagner H. D.: Tensile mechanics of electrospun multiwalled nanotube/poly(methyl methacrylate) nanofibers. *Advanced Materials*, **19**, 1228–1233 (2007).
DOI: [10.1002/adma.200602226](https://doi.org/10.1002/adma.200602226)
- [27] Yuya P. A., Wen Y. K., Turner J. A., Dzenis Y. A., Li Z.: Determination of Young's modulus of individual electrospun nanofibers by microcantilever vibration method. *Applied Physics Letters*, **90**, 111909/1–111909/3 (2007).
DOI: [10.1063/1.2713128](https://doi.org/10.1063/1.2713128)
- [28] Gu S-Y., Wu Q-L., Ren J., Vancso G. J.: Mechanical properties of a single electrospun fiber and its structures. *Macromolecular Rapid Communications*, **26**, 716–720 (2005).
DOI: [10.1002/marc.200400667](https://doi.org/10.1002/marc.200400667)
- [29] Callister W. D.: *Materials science and engineering: An introduction*. Wiley, New York (2003).